XA0102603

DEVELOPMENT OF IRRADIATED UO_2 THERMAL CONDUCTIVITY MODEL

CHAN BOCK LEE, JE-GEON BANG, DAE HO KIM, YOUN HO JUNG
Korea Atomic Energy Research Institute,
Taejon, Republic of Korea

Abstract

Thermal conductivity model of the irradiated UO_2 pellet was developed, based upon the thermal diffusivity data of the irradiated UO_2 pellet measured during thermal cycling. The model predicts the thermal conductivity by multiplying such separate correction factors as solid fission products, gaseous fission products, radiation damage and porosity. The developed model was validated by comparison with the variation of the measured thermal diffusivity data during thermal cycling and prediction of other UO_2 thermal conductivity models. Since the developed model considers the effect of gaseous fission products as a separate factor, it can predict variation of thermal conductivity in the rim region of high burnup UO_2 pellet where the fission gases in the matrix are precipitated into bubbles, indicating that decrease of thermal conductivity by bubble precipitation in rim region would be significantly compensated by the enhancing effect of fission gas depletion in the UO_2 matrix.

1. INTRODUCTION

Thermal conductivity of UO_2 pellet depends upon such variables as density, porosity, stoichiometry, temperature and impurities. In addition, under irradiation condition, it is affected by radiation damage and fission product buildup. Thermal conduction of UO_2 pellet occurs mainly via phonon transport at the temperature below 1500°C, and at the temperature higher than 1500℃ thermal conduction by free electrons is added to the phonon transport. In UO_2 of ceramic lattice structure, thermal conduction by free electrons increases with temperature since mobility of free electrons increases with temperature. Thermal conduction by phonon transport is like hypothetical quantum particle transport through the solid lattice structure that also has the wave characteristics. Since vibration of atoms in the lattice increases with temperature, thermal resistance increases with temperature due to the interference with phonon wave. Lattice defects such as point defect, line defect and loop, and impurities also interfere with the phonon waves to decrease the thermal conductivity. Capability to scatter the phonon wave is known to be in the order of point defect, line defect and bubbles or large precipitates of fission product compound [1].

2. ANALYSIS OF UO_2 THERMAL CONDUCTIVITY MODELS

2.1. Variables

Porosity

Effect of porosity upon the thermal conductivity depends upon the shape and distribution of the pores. Porosity consists of the pores formed during the UO_2 pellet manufacturing and fission gas bubbles formed during the irradiation. Fission gas bubbles at the grain boundary have lenticular shape due to the surface effect of the grain boundary while the bubbles inside the grain and in the rim region of the high burnup UO_2 fuel are sphere. Pores formed during UO_2 manufacturing have irregular shape and surfaces. There are various porosity correction correlations available as shown below [2]. Thermal conductivity of the inner gases of the bubbles and the pores is too small compared with that of the UO_2 matrix, so that thermal conduction through the pores can be neglected.

- Loeb correlation: $f_p = 1 - \alpha p$
- Maxwell correlation: $f_p = (1-p)^{1.5}$
- Maxwell-Eucken correlation: $f_p = (1-p)/(1 + \beta p)$
- Schulz correlation: $f_p = (1-1.5p)$
- Bakker correlation: $fp = (1-p)^{1.7 \pm 0.7}$.

Values of α and β factors in Loeb and Maxwell-Eucken correlations is theoretically 1 and 0.5, respectively when the pore is sphere and uniformly distributed. However, fitting of the measured thermal conductivity of the unirradiated UO_2 showed that α is 2.5 $\pm$ 1.5, which means that reduction of the thermal conductivity is more enhanced due to the irregular shape and non-uniform distribution of the pores. Schulz correlation was analytically derived for the case of the sphere pores and uniform pore distribution. Bakker correlation was derived by finite element analysis of the actual pore and bubble distribution of 25 MWD/kgU irradiated fuel [3]. Fig. 1 compares different porosity correction correlations. It can be seen that decrease of thermal conductivity by porosity is enhanced in proportion to deviation from sphere in pore shape and deviation from uniformity in pore distribution.

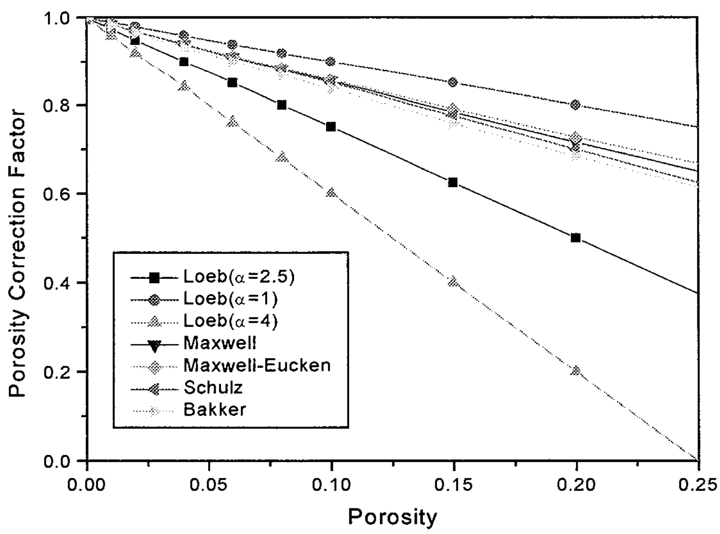

Fig. 1. Porosity Correction Factor.

Fission Products

Fission products exist mostly as four different states in UO_2 as follows [4].

- Dissolved in the matrix as an oxide: Sr, Zr, Nb, Y, La, Ce, Pr, Nd, Pm, Sm
- Metallic precipitate:: Mo, Tc, Ru, Rh, Pd, Ag, Cd, In, Sb, Te
- Oxide precipitate: Ba, Zr, Nb, Mo, (Rb, Cs, Te)
- Gas and volatile elements: Kr, Xe, Br, I, (Rb, Cs, Te).

Effect of fission products upon the UO_2 thermal conductivity were studied extensively by using SIMFUEL which simulates the irradiated fuel by mixing the non-radioactive fission product elements [5]. Thermal conductivity measurement of SIMFUEL showed that metallic precipitates (0.05 ~ 1 μm) increase the thermal conductivity of UO_2 due to higher thermal conductivity of metallic precipitates than UO_2 matrix while other fission products decreases UO_2 thermal conductivity [6].

Impurities and Additives

Impurities or additives in UO_2 decrease thermal conductivity like fission products. Thermal conductivity of UO_2/Gd_2O_3 decreases with the content of Gd_2O_3. Gd_2O_3 is body centered cubic structure so that it may deform lattice structure of UO_2 and enhance the defect formation in UO_2 of face-center cubic structure. In addition, Gd_2O_3 changes the phonon-phonon scattering characteristic due to the mass difference between Gd_2O_3 and UO_2 [7].

Stoichiometry

Measured thermal conductivity of $UO_{2\pm x}$ showed that thermal conductivity would be decreased for hyper-stoichiometry($x > 0$) while it is slightly increased for hypo-stoichiometry($x < 0$). However, for the irradiated UO_2, effect of stoichiometry can not be simply separated from the fission product buildup due to fission of uranium element so that it should be taken into account along with the effect of the fission products or burnup. Therefore, thermal conductivity model for the irradiated UO_2 mostly does not consider the effect of stoichiometry as an independent factor.

Radiation Damage

Under the irradiation condition, radiation damage such as point defects, dislocation and loops are formed in UO_2. Those defects decrease thermal conductivity by interference with the phonon wave. As temperature increases, level of radiation damage decreases due to annealing of the radiation defects. Point and line defects are known to be annealed by recombination below 1000 K [10]. Radiation damage becomes saturated at lower burnup so that amount of radiation damage does not increase linearly with the burnup.

2.2. Analysis of UO_2 Thermal Conductivity Models

Lucuta Model [6]

Lucuta model for the irradiated UO_2 published in 1996 is as follows.

$$\lambda = K_{1d}K_{1p}K_{2p}K_{3x}K_{4r}\lambda_0$$

$$\lambda_0 = \frac{1}{(0.0375 + 2.165\times10^{-4}\cdot T)} + \frac{4.715\times10^{9}}{T^2}\exp(-\frac{16361}{T})$$

where,

λ = thermal conductivity of irradiated UO_2
λ_0 = thermal conductivity of unirradiated 100% dense UO_2
K_{1d} = factor for fission products
K_{1p} = factor for precipitated metal fission products
K_{2p} = factor for porosity
K_{3x} = factor for stoichiometry
K_{4r} = factor for radiation damage.

Effect of fission products is based upon the test results of SIMFUEL. Daniel and Cohen's data [11] were used for the effect of radiation damage. Maxwell-Eucken correlation was used for porosity correction and Harding and Martin data [12] are used for thermal conductivity of 100% UO_2 .

2.2.1. Halden Model [8]

Halden model is based upon the in-pile measured data of fuel centerline temperature in relation to power level. It has been continuously improved by adjusting the model constants as the new measured data are generated. Halden model published in 1997 is as follows.

$$\lambda_{95} = \frac{1}{0.1148 + 0.0035BU + 2.475\times10^{-4}(1-0.00333BU)T} + 0.0132\exp(0.00188T)$$

where λ_{95} is thermal conductivity of unirradiated 95% UO_2 (w/m.K), BU is burnup(MWD/kgU) and T is temperature (^oC). Halden model is considered to directly represent the in-pile thermal conductivity of UO_2 since it is based upon in-pile measured temperature data. However, since the temperature was measured only at the fuel center, it may not fully represent the wide range of radial temperature variation in the fuel and there may be somewhat uncertainties in the fuel gap conductance.

2.2.2. NFI Model [9]

NFI model was developed based upon the thermal diffusivity data of 61 MWD/kgU UO_2 fuel measured by laser flash technique. Thermal conductivity of UO_2 can be deduced from its relation with thermal diffusivity, density and heat capacity. NFI model is as follows.

$$\lambda_{95} = \frac{1}{4.52\times10^{-2} + 2.46\times10^{-4}T + 1.87\times10^{-3}BU + 0.038BU^{0.28}\cdot h(T)} - 5.47\times10^{-9}T^2 + 2.29\times10^{-14}T^4$$

$$h(T) = \frac{1}{1+396\exp(-6380/T)}$$

where λ_{95} is thermal conductivity of unirradiated 95% TD UO_2 (w/m.K), BU is burnup (MWD/kgU), T is temperature (K), and h (T) represents the effect of radiation damage.

3. DEVELOPMENT OF UO_2 THERMAL CONDUCTIVITY MODEL

3.1. Model Development

In NFIR (Nuclear Fuel Industry Research) Program managed by EPRI, thermal diffusivity of irradiated UO_2 fuel was measured by laser flash technique by changing temperature [13,14]. There were three different irradiated fuel specimens with the burnup of 24.9 MWD/kgU (U2), 36.23 MWD/kgU (U4) and 59.93 MWD/kgU (U6), respectively. Table 1 shows the temperature histories during thermal diffusivity measurement.

Thermal diffusivity was measured at every 100°C from 300°C to 1600°C. Measured data during cycle 1 may represent the thermal diffusivity of the specimen with all the effects accumulated during irradiation. After cycle 1 of maximum temperature of 800°C and cycle 2 of maximum temperature of 1100°C, it may be assumed that all the radiation damage was

TABLE 1. HISTORY OF THERMAL CYCLING OF THE SPECIMENS

Cycle	Temperature (°C)			Duration of Cycle of Specimen (min)		
	Initial	Peak	Final	U2	U4	U6
1	300	800	300	269	330	332
2	300	1100	500	240	375	485
3	500	1500	300	422	412	485
4	300	1600	300	469	542	611

annealed out. Therefore, the data measured during cycle 3 may represent thermal diffusivity of irradiated fuel with the effect of fission products except radiation damage. After cycle 3 of maximum temperature of 1500°C, it may be assumed that fission gas atoms in the matrix would be released out of fuel or precipitated into fission gas bubble so that there may be no fission gas atoms left in the matrix. Therefore, measured data during cycle 4 may represent the thermal diffusivity of irradiated fuel with only the effect of solid fission products. The fact that there is not much difference between thermal diffusivity data measured during cycles 3 and 4 [13, 14] indicates that fission gas atoms in the matrix may have been mostly depleted during cycle 3.

Examination of the microstructure of the specimens after thermal cycling [14] showed that there were bubbles of micron size at the grain boundary for U4 specimen. For the high burnup specimen of U6, micron size bubble were found both at the grain boundary and inside the grain, and size of the bubbles increased near the periphery of the specimen due to the higher burnup in that region.

Separate effects of such variables as solid fission product, fission gas and radiation damage can be deduced from the variation of the thermal diffusivity during thermal cycling. Therefore, thermal conductivity model was derived from the measured thermal diffusivity data by considering the effects of solid fission product, fission gas and radiation damage as a separate factor, which is similar to Lucuta model. Those factors were derived by fitting the measured thermal diffusivity data. Since the porosity data of the irradiated UO_2 fuel specimens before and after the thermal cycling were not available, porosity variation during thermal cycling could not be considered.

$$\lambda = f_{sfp} f_{fg} f_{rd} f_p \lambda_0$$

$$f_{sfp} = \frac{10.152 + 0.0762T}{10.152 - 4.8054BU^{0.5} + 1.563BU + (0.0762 + 4.724\times10^{-3}BU^{0.5} - 8.624\times10^{-4}BU)\cdot T}$$

$$f_{fg} = \frac{10.152 - 4.8054BU^{0.5} + 1.563BU + (0.0762 + 4.724\times10^{-3}BU^{0.5} - 8.624\times10^{-4}BU)\cdot T}{10.152 - 1.423BU^{0.5} + 1.6072BU + (0.0762 + 3.043\times10^{-3}BU^{0.5} - 8.066\times10^{-4}BU)\cdot T}$$

$$f_{rd} = \frac{1}{4.0413\exp(31.598/T) - 3.1186}$$

$$\lambda_0 = \frac{1}{(0.0375 + 2.165\times10^{-4}\cdot T)} + \frac{4.715\times10^{9}}{T^2}\exp(-\frac{16361}{T})$$

where,

λ = thermal conductivity of irradiated UO_2

λ_0 = thermal conductivity of unirradiated 100% dense UO_2

f_{sfp} = factor for solid fission products

f_{fg} = factor for gaseous fission products

f_{rd} = factor for radiation damage

f_p = factor for porosity

T = temperature (K)

B = burnup (MWD/kgU).

Figs 2-4 compare the prediction results of solid fission product factor, gaseous fission product factor and radiation damage factor with the results derived from the measured thermal diffusivity data during thermal cycling, respectively. It can be seen that there is somewhat scattering in the fission gas factor. Dependency of fission gas factor upon the burnup seems to be smaller than that of the solid fission products factor. Radiation damage factor seems to be independent of the burnup since its effect may be saturated at low burnup. It can be seen that radiation damage is annealed at temperature above 1100^{oC}. Fig. 5 compares prediction of the burnup factor which is defined as multiplication of solid fission product, gaseous fission product and radiation damage, with the measured data. Except the scattering of the measured data above 1300°C, the model reproduced the measured thermal conductivity quite well.

Figs 6-9 compare the developed model prediction with prediction of Lucuta, Halden and NFI models. Developed model is closer to NFI model since both models were derived from the measured thermal diffusivity data of the irradiated UO_2 fuel. Halden model over-estimates the thermal conductivity at low temperature, which indicates that Halden model may not fully consider the effect of radiation damage at low temperature since the measure in-pile centerline temperature and fuel average temperature is somewhat higher [1]. Lucuta model has a separate factor for the metallic fission product precipitates which increases thermal conductivity, so that it generally over-estimates the thermal conductivity and, compared with other models, decrease rate of thermal conductivity with temperature is low between 500^{oC} and 800^{oC}.

3.2. Application to UO_2 rim region

Since the developed model takes into account the effect of fission gas as a separate factor, it can be directly applied to the prediction of thermal conductivity in high burnup UO_2 rim region where fission gas atoms in the matrix are depleted to be precipitated into fission gas bubbles with the porosity of 15–17% [15, 16]. Thermal conductivity in UO_2 rim region can be obtained by

$$\lambda_{rim} = f_{sfp}^{rim} f_{rd} f_p^{rim} \lambda_0.$$

Fission gas bubbles in rim region are sphere shape and uniformly distributed, so that Schulz correlation can be used for porosity correction. As an example, it was applied to thermal conductivity in the UO_2 rim region where bubble porosity is 15% and local burnup of 80 MWD/kgU at 600^{oC}, in comparison with that of normal UO_2 where fission gases are still in the matrix without fission gas bubble. In rim region, thermal conductivity is increased by 18% due to the depletion of fission gases from the matrix while it is reduced by 23% due to the porosity of 15% according to Schulz correlation. Therefore, compared with normal UO_2 at same burnup, net decrease of thermal conductivity in the UO_2 rim region due to fission gas bubble precipitation may be only about 9% for this case. It indicates that decrease of thermal conductivity by fission gas bubble precipitation in the UO_2 rim region would be significantly compensated by the enhancing effect of fission gas depletion in the UO_2 matrix.

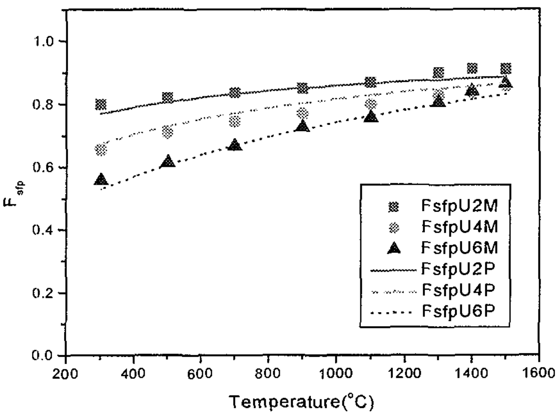

*Fig. 2. Solid fission product factor (*M: Measured, *P: Prediction).*

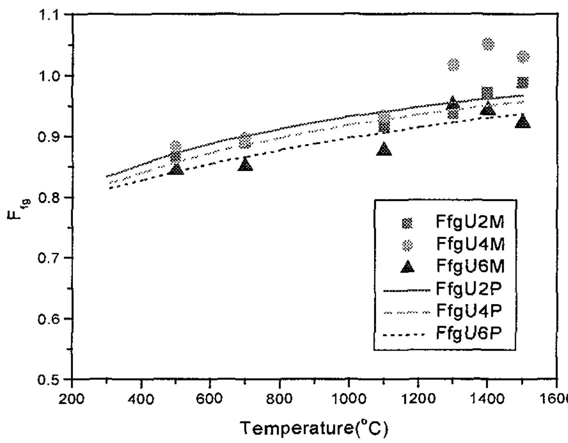

*Fig. 3. Gaseous fission product factor (*M: Measured, *P: Prediction).*

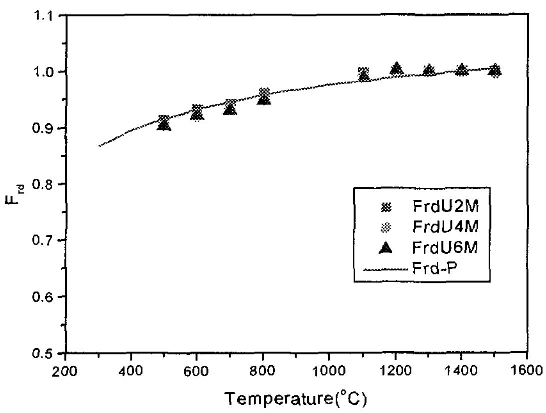

*Fig. 4. Radiation damage factor (*M: Measured, *P: Prediction).*

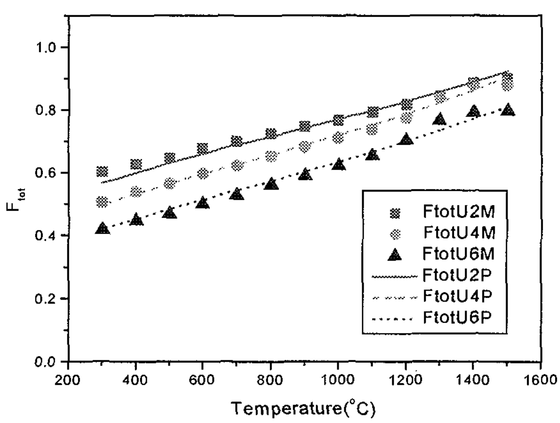

*Fig. 5. Burnup factor (*M: Measured, *P: Prediction).*

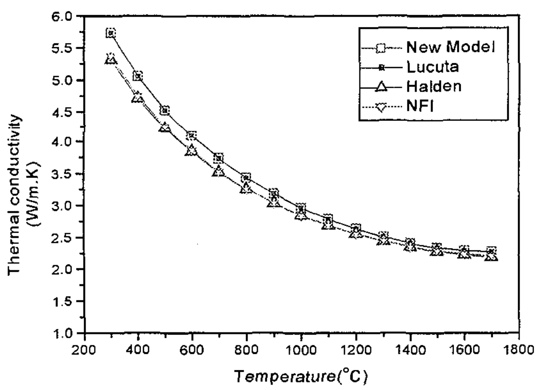

Fig. 6. Thermal conductivity of unirradiated (95% TD)% UO_2.

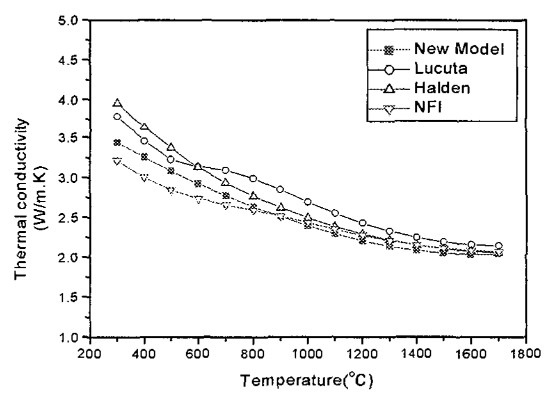

Fig. 7. Thermal conductivity of 20 MWD/kgU.

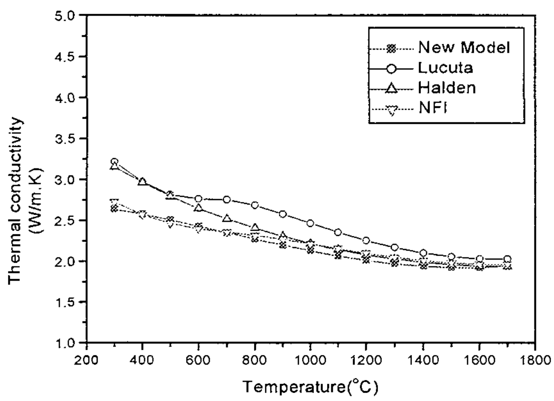

Fig. 8. Thermal conductivity of 40 MWD/kgU.

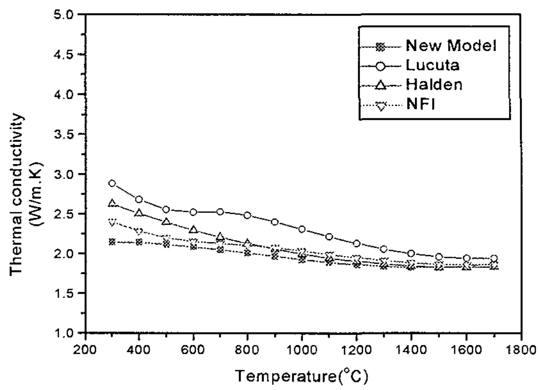

Fig. 9. Thermal conductivity of 60 MWD/kg UO_2.

4. CONCLUSION

Thermal conductivity model of the irradiated UO_2 pellet was developed, based upon the thermal diffusivity data of the irradiated UO_2 pellet measured during thermal cycling. The model predicts the thermal conductivity by multiplying such separate factors as solid fission products, gaseous fission products, radiation damage and porosity.

The developed model was validated by comparison with both the variation of the measured thermal diffusivity data during thermal cycling and the prediction of other UO_2 thermal conductivity models.

Since the developed model considers the effect of gaseous fission products as a separate factor, it can predict variation of thermal conductivity in the rim region of high burnup UO_2 pellet where the fission gases in the matrix are precipitated into the bubbles, indicating that decrease of thermal conductivity by bubble precipitation in rim region would be significantly compensated by enhancing effect of fission gas depletion in the UO_2 matrix.

ACKNOWLEDGEMENT

This work has been carried out under the Nuclear R&D Program supported by Ministry of Science and Technology in Korea. Thermal diffusivity data of the irradiated UO_2 fuel were generated in NFIR (Nuclear Fuel Industry Research) Program managed by EPRI. The authors would like to thank Dr. S. K. Yagnik for review of manuscript and helpful comments.

REFERENCES

[1] C. BEYER and D. LANNING, "Review of fuel thermal conductivity data and model", Seminar on Thermal Performance of high burnup LWR Fuel, Cadarache, France, 2-6 March, 1998.

[2] D.G. MARTIN, "A Re-appraisal of the thermal conductivity of UO_2 and mixed (U,Pu) oxide fuel", J. Nucl. Mater. 110 (1982) 73.

[3] K. BAKKER, et al., "Determination of a porosity correction factor for the thermal conductivity of irradiated UO_2 fuel by means of the finite element method", J. Nucl. Mater. 226 (1995) 128.
[4] H. KLEYKAMP, "The chemical state of the fission products in oxide fuels", J. Nucl. Mater. 131 (1985) 221.
[5] P.G. LUCUTA, et al., "Modelling of UO_2-based SIMFUEL thermal conductivity: The effect of the burnup", J. Nucl. Mater. 217 (1994) 279.
[6] P.G. LUCUTA, et al., "A pragmatic approach to modeling thermal conductivity of irradiated UO2 fuel: review and recommendations", J. Nucl. Mater. 232 (1996) 166.
[7] D. BARON and J.C. COUTY, "A proposal for a unified fuel thermal conductivity model available for UO_2, $(U\text{-}Pu)O_2$ and UO_2-Gd_2O_3 PWR fuel", IAEA-TECDOC-957, 1997.
[8] W. WIESENACK, "Assessment of UO_2 conductivity degradation based upon in-pile temperature data", Proc. of Int. Top. Mtg. on LWR Fuel Performance, Portland, Oregon, 1997.
[9] K. OHIRA and N. ITAKI, "Thermal conductivity measurements of high burnup UO_2 pellet and a benchmark calculation of fuel temperature", Proc. of Int. Top. Mtg. on LWR Fuel Performance, Portland, Oregon, 1997.
[10] M. AMAYA and M. HIRAI, "Recovery behavior of thermal conductivity in irradiated UO_2 pellets", J. Nucl. Mater. 247 (1997) 76.
[11] R.C. DANIEL and I. COHEN, "In-pile effective thermal conductivity of oxide fuel elements to high burnup depletion", WAPD-246, 1964.
[12] J.H. HARDING and D.G. MARTIN, "Recommendation for the thermal conductivity of UO_2", J. Nucl. Mater. 166 (1989) 166.
[13] S. YAGNIK, "Thermal conductivity recovery phenomenon in irradiated UO_2 and $(U,Gd)O_2$", Proc. of Int. Top. Mtg. on LWR Fuel Performance, Parkcity, Utah, 2000.
[14] M. LIPPENS and L. MERTENS, "High burnup UO_2 and $(U,Gd)O_2$ thermal diffusivity measurements and post-irradiation characterizations", EPRI Report TR-106501, 1996.
[15] J. SPINPO, et al., "Detailed characterization of the rim microstructure in PWR fuels in the burnup range 40-67 GWd/tM", J. Nucl. Mater. 231 (1996) 179.
[16] J. SPINO, et al., "High burnup rim structure: evidences that xenon-depletion, pore formation and grain subdivision strat at different local burnups", J. Nucl. Mater. 256 (1998) 189.